

Superposition and higher-order spacing ratios in random matrix theory

Udaysinh T. Bhosale*

Physical Research Laboratory, Navrangpura, Ahmedabad 380 009, India

(Dated: May 10, 2019)

The joint distribution of every second eigenvalue obtained after superposing the spectra of two circular orthogonal ensembles ($\beta = 1$) is known to be equal to that of the circular unitary ensemble ($\beta = 2$), where the parameter β is the Dyson index of the ensemble. Superposition of spectra of m such circular orthogonal ensembles is studied numerically using higher-order spacing ratios. It is conjectured that the joint probability distribution of every $k = m - 2$ -th ($m \geq 4$) eigenvalue corresponds to that of circular β -ensemble with $\beta = m - 3$. For the special case of $m = 3$, $k = \beta = 3$. It is also conjectured that the spectral fluctuations corresponding to $k = m + 1$ ($m \geq 2$) and $k = m - 3$ -th ($m \geq 5$) order spacing ratio distribution is identical to that of nearest neighbor spacing ratio distribution with Dyson indices $m + 2$ and $m - 4$ respectively. Strong numerical evidence in support of these conjectures is presented.

I. INTRODUCTION

Superposition principle has played an important role in our understanding of classical and quantum physics. The famous Young's double slit experiment has been explained using this principle. In quantum physics, since Schrodinger equation is linear, the superposition of its solutions can be used to get new ones. In quantum information theory, superposition of states can create or destroy entanglement [1]. In similar ways, superposition of eigenvalues of random matrices can lead to different fluctuation properties [2–6]. Superposition of eigenvalues can also occur if a given matrix H possess an additional symmetry S , i.e. $[H, S] = 0$. This splits the Hilbert space of the system into invariant subspaces. In other words, the H becomes block diagonal in the basis formed by the eigenfunctions of S , i.e., $H = H_1 \otimes H_2 \otimes \dots \otimes H_m$. Here, m denotes the number of non-degenerate eigenvalues of S . Thus, due to the symmetry S , in the spectra of H the eigenvalues from different blocks get superposed. Symmetries have played an important role in our understanding of many areas of physics [7–9]. The importance of symmetries can be understood from the works of Emmy Noether, where she has related continuous symmetry and conservation laws in her famous theorem.

Symmetries have also played an important role in the random matrix theory (RMT) [4, 10]. This goes back to Wigner who defined a class of Gaussian random matrix ensembles to understand the fluctuations in nuclear spectra. The class of ensemble one uses depends on the symmetry present in the system. In RMT, the spectral fluctuations are modeled using the most popular measure namely the nearest neighbour (NN) level spacings, $s_i = E_{i+1} - E_i$, where E_i , $i = 1, 2, \dots$ are the eigenvalues of the Hamiltonian H . Wigner surmised that in time-reversal invariant systems without a spin degree of freedom, these spacings are distributed as $P(s) = (\pi/2)s \exp(-\pi s^2/4)$, which indicates the level re-

pulsion. For these systems, the statistical properties of the spectra are modelled correctly by the Gaussian Orthogonal Ensemble (GOE) having Dyson index $\beta = 1$. Other ensembles that are used commonly in RMT are Gaussian unitary ensemble (GUE) and Gaussian symplectic ensemble (GSE) having Dyson index $\beta = 2$ and 4 respectively. In this work, we use circular class of ensembles for our study [10]. The symmetries that are used in defining respective Gaussian ensembles are the same for those of circular ensembles. Indices $\beta = 1, 2$ and 4 corresponds to Dyson's threefold way and have played an important in physics. Matrix representation for these indices was given in the initial development of RMT. But these ensembles are valid and exists for continuous parameter $\beta \in (0, \infty)$ and a tridiagonal random matrix model have been defined for them [11]. It has been used recently in the study of level statistics of many-body localization for $\beta \in (0, 1]$ [12]. The index β is interpreted as the inverse temperature of $T = 1/\beta$ in the RMT literature.

The Wigner's surmise has been extended to all quantum chaotic systems in the form of Bohigas-Giannoni-Schmidt conjecture [13], which states that such systems display level statistics consistent with that of an appropriately chosen random matrix ensemble. Due to the additional symmetry S , the eigenvalues from different blocks get superposed. This results in level clustering and one obtains the spacings distribution to be Poissonian [4], $P(s) = \exp(-s)$, which also corresponds to the spectral fluctuations of integrable systems [14]. This implies that to study genuine spectral correlations, the eigenvalues must be drawn from the same subspace.

Motivated by the works of Wigner, Dyson introduced new class of ensembles of random matrices known as circular β -ensembles which are measures of the spaces of unitary matrices [15]. They have played important roles in RMT. The Dyson index $\beta = 1, 2$ and 4 corresponds to Circular Orthogonal Ensemble (COE), Circular Unitary Ensemble (CUE) and Circular Symplectic Ensemble (CSE) respectively. These ensembles have found applications in the scattering from a disordered cavity [10], condensed matter and optical physics [16]. Algorithm for generating these ensembles numerically is non triv-

*Electronic address: udaybhosale0786@gmail.com

ial compared to that of Gaussian ensembles and is given in Ref.[17]. Similar to Gaussian β -ensemble, the circular β -ensemble is also defined for continuous parameter $\beta \in (0, \infty)$ and a corresponding tridiagonal model is defined for them [5, 18].

Previous studies have shown connections within ensembles corresponding to $\beta = 1, 2$ and 4 . A theorem which relates the properties of the CUE and COE has been conjectured in Ref.[2] and later proved by Gunson [3]. It states that the alternate eigenvalues obtained after superposition of spectra of two matrices of same dimension from COE belongs to that of CUE. A similar theorem relating properties of COE and CSE were proved in Ref.[19]. It states that, the alternate eigenvalues of an even dimensional COE belongs to that of CSE. Thus, these two theorems together state that all the statistical properties of the three ensembles are derivable from that of COE alone [19]. In fact, these two theorems hold at the level of joint probability distribution function (jpdf). A natural question that can be asked as follows: Can these two theorems be generalized to obtain circular ensembles with other values of β ? There are recent studies in this direction at the level of spectral fluctuations but not at the level of jpdf [6]. There it is shown that when m number of COE spectra are superposed then the distribution of the m -th order spacing ratios is same as that of NN spacing ratios of circular ensemble with Dyson index m . (The definition of higher-order spacing ratios will be given in detail in Sec.II). In the same paper Ref.[6], this result is then used for deducting symmetries in various complex systems.

In this work, we present rigorous numerical evidence for the generalization of the theorem relating superposition of spectra of two COEs resulting in a CUE ensemble [2, 3]. In fact, our conjecture relates the jpdf of the circular ensemble with positive integer-valued β to the superposition of COEs. We have also studied the spectral fluctuations on the lines of Ref.[6]. It is shown that after superposing m number of COE spectra, the distribution of $m + 1$ and $m - 3$ -th order spacing ratios are related to that of NN spacing ratios of circular ensemble with Dyson index β' , where β' is given in terms of m .

The structure of the paper is as follows: In Sec.II definition of various quantities, namely, the NN spacing ratios, higher-order spacing ratios are given. Previous studies from random matrix theory and other fields using these definitions are presented. In Sec.III our results using the higher-order spacing ratios of superposition of COEs are presented. Numerical evidence in support of our results are presented. In Sec.IV summary of our results and conclusion is given.

II. PRELIMINARIES

For the study of the spacing distribution, one needs to do the unfolding of the spectra which removes the system dependent spectral features, i.e., the average part of the

k	$\beta = 1$	$\beta = 2$	$\beta = 3$	$\beta = 4$
1	1	2	3	4
2	4	7	10	13
3	8	14	20	26
4	13	23	33	43
5	19	34	49	64
6	26	47	68	89
7	34	62	90	118
8	43	79	115	151

TABLE I: Tabulation of higher-order indices β' for various k and β using Eq. (3).

density of states [4, 20]. This procedure is nonunique and cumbersome in many cases. This difficulty can be solved by using the NN spacing ratios [21], i.e., $r_i = s_{i+1}/s_i$, $i = 1, 2, \dots$, since it is independent of the local density of states and thus does not require unfolding. The distribution of r_i , $P(r)$ has been obtained for Gaussian ensembles and is given as follows [22, 23]:

$$P(r, \beta) = \frac{1}{Z_\beta} \frac{(r + r^2)^\beta}{(1 + r + r^2)^{(1+3\beta/2)}}, \quad \beta = 1, 2, 4 \quad (1)$$

where Z_β is the normalization constant that depends on β . This quantity has found many applications, like numerical investigation of many-body localization [12, 21, 24–28], localization in constrained quantum system [29], quantifying the distance from integrability on finite size lattices [30–34] and to study localization transition in Lévy matrices [35].

Variations of the spacing ratios have been studied in the recent past [23, 36–38]. In this work, we consider the non-overlapping k -th order spacing ratio, where no eigenvalue is shared between the spacings of numerator and denominator, defined as follows:

$$r_i^{(k)} = \frac{s_{i+k}^{(k)}}{s_i^{(k)}} = \frac{E_{i+2k} - E_{i+k}}{E_{i+k} - E_i}, \quad i, k = 1, 2, 3, \dots \quad (2)$$

This ratio has been used to study higher-order fluctuation statistics in the Gaussian [39] and Wishart ensembles [40], and a scaling relation is given as follows:

$$P^k(r, \beta, m = 1) = P(r, \beta'), \quad \beta = 1, 2, 4 \quad (3)$$

$$\beta' = \frac{k(k+1)}{2} \beta + (k-1), \quad k \geq 1.$$

It tells that the distribution of k -th order spacing ratio for a given β ensemble is the same as that of NN spacing ratios of $\beta'(> \beta)$ ensemble. It has been applied successfully to various physical systems like spin chains, chaotic billiards, Floquet systems, observed stock market, etc. [39, 40]. It is also used recently to find the symmetries in complex systems [6]. In Ref.[6] (as explained in the Introduction) the distribution of the m -th order spacing ratios after superposing the spectra of m COEs is studied. It is shown to be converging to the distribution of

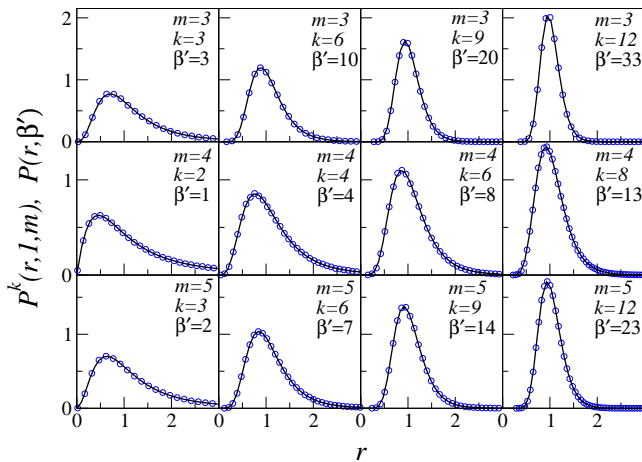


FIG. 1: (Color online) Distribution of the k -th order spacing ratios (circles) for a superposition of m COE spectra. For $m = 3$ and 4 the dimension of the matrices is $N = 8400$ and for $m = 5$ it is 9000 . The solid curve corresponds to $P_{\text{num}}(r, \beta')$ as given in Eq.(9). Here, $\beta' = \frac{k'(k'+1)}{2}\beta + k' - 1$ where $k' = k/(m-2)$ and $\beta = m-3$ for $m \geq 4$. While $k' = k/3$ and $\beta = 3$ for $m = 3$.

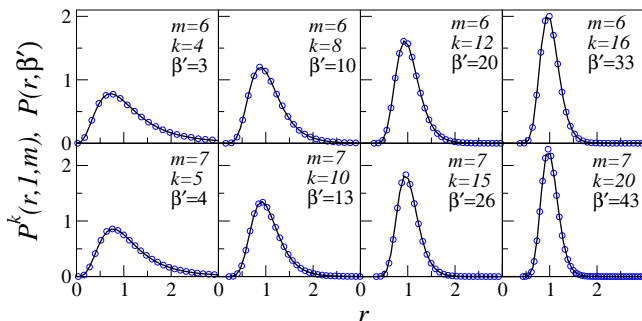


FIG. 2: (Color online) Same as that of Fig.1 but for $m = 6$ and 7 . Here, $N = 8400$.

the NN spacing ratios $P(r, \beta')$ with $\beta' = m$ i.e.

$$P^k(r, 1, m) = P(r, \beta'), \text{ where } \beta' = k = m. \quad (4)$$

The Eq. (3) is tabulated for few values of β and k in Table I. It can be observed from the $\beta = 1$ series in Table I that the $\beta = 4$ series appears at its even places. This is because of the relation between COE and CSE exists at the level of the jpdf of the eigenvalues [2, 3]. This observation plays an important role in further analysis in the subsequent part of this paper. The special case of the Eq. (3) for $0 \leq \beta \leq 1$ is given in Refs.[41, 42] that too at the level of the joint probability distribution of eigenvalues. There, it is shown that the jpdf of every k -th eigenvalue in certain β -ensembles with $\beta = 2/k$ is equal to that of another β -ensemble with $\beta = 2k$.

III. RESULTS

In this work, our main object of study is the circular β -ensembles. The jpdf is given as follows:

$$Q_{N,\beta}[\{\theta_i\}] = C_{N,\beta} \prod_{k>j}^N |\exp(i\theta_j) - \exp(i\theta_k)|^\beta \quad (5)$$

where N is the dimension and $C_{\beta,N} = (2\pi)^{-N} \{\Gamma(1 + \beta/2)\}^N \{\Gamma(1 + N\beta/2)\}^{-1}$ is the normalization constant [4, 10]. The eigenvalues θ_i lies on the unit circle and display level repulsion [4].

Based on numerical simulations the main results or conjectures of this work are now summarized.

1. If $m \geq 4$ independent spectra of COE are superposed, then upon integrating all the eigenvalues except every $k = m-2$ -th one, gives the jpdf of circular β' -ensemble with $\beta' = m-3$. For the special case when $m = 3$, we have $k = \beta' = 3$. Thus,

$$Q_{N,1}^k[\{\theta_i\}, m] = Q_{N',\beta'}[\{\theta_i\}] \text{ where } k = m-2, \quad (6)$$

$$\beta' = m-3 \text{ and } N' = mN/(m-2).$$

Here, N has to be chosen such that N' is an integer. For the case $m = 3$, we have $N' = N$. The condition on the value of N is motivated from Refs.[3, 19, 43]. To understand this, without loss of generality, the eigenvalues can be arranged in ascending order, so that $0 < \theta_1 < \theta_2 < \dots < \theta_{mN} < 2\pi$. Thus, when one starts to select every k -th ($= m-2$) eigenvalue starting from, say θ_1 , then one obtains the sequence $\{\theta_1, \theta_{k+1}, \theta_{2k+1}, \theta_{3k+1}, \dots, \theta_{(N'-1)k+1}\}$. Thus, the condition on N makes sure that the next value in the sequence which is $\theta_{N'k+1}$ equals θ_{mN+1} , which is equal to θ_1 , since all the eigenvalues lie on the circle.

2. Two different relations on the lines of Eq.(4) (see Ref.[6]) at the level of spectral fluctuations are obtained. The first relation is as follows:

$$P^k(r, 1, m) = P(r, \beta'), \text{ for } \beta' = k+1 = m+2 \quad (7)$$

and $m \geq 2$, while the second one is as follows:

$$P^k(r, 1, m) = P(r, \beta'), \text{ for } \beta' = k-1 = m-4 \quad (8)$$

and $m \geq 5$. This result is asymptotic in N . Except this there is no condition on the value of N since these equations are only relating the fluctuations of the ensembles.

Now various numerical evidences supporting our conjectures are presented. The numerical simulations in support of the conjecture in Eq. (6) are presented in Figs.1 and 2. It can be seen that, if the conjecture is correct then for given m , every $k = m-2$, $k = 2(m-2)$, $k = 3(m-2)$,

...-th eigenvalue will give the spacing ratio as per the series in Eq. (3) for $\beta' = m - 3$ (see Table I for the specific values). This can be observed in Figs.1 and 2. For numerical simulations, the value of N is taken such that it is multiple of least common multiple of numbers from 2 to 9. For $m = 5$ we have taken $N = 9000$ for rest $N = 8400$. These dimensions make sure that N'/i ($i = 1$ to 4) remains a whole number. Here, i corresponds to column number in the figures.

Motivated by the work in Ref.[22], in order to get the best fit as shown in Figs. 1 and 2, we have gone beyond the surmise in Eq. (3) for the higher-order spacing ratios, though the deviations (not shown here) from the surmise are very small (the analysis just using Eq. (3) is also carried out and is discussed in the subsequent part of the paper). The numerical fits in these figures are given by

$$P_{\text{num}}(r, \beta, m) = P(r, \beta') + \delta P_{\text{fit}}(r, \beta', m). \quad (9)$$

Here,

$$\delta P_{\text{fit}}(r, \beta', m) = \frac{C_{\beta', m}}{(1+r)^2} \left[\left(r + \frac{1}{r} \right)^{-\beta'} - c_{\beta'} \left(r + \frac{1}{r} \right)^{-(\beta'+1)} \right] \quad (10)$$

where $c_{\beta'}$ is calculated using the normalization condition $\int_0^\infty \delta P_{\text{fit}}(r, \beta') dr = 0$ (see Table II for the approximate numerical values. For exact values refer Appendix A). The same form for $\delta P_{\text{fit}}(r, \beta')$ has been used earlier in Ref.[22] while studying the NN spacings ratios. The form for δP_{fit} is surmised on the assumption that $P_{\text{num}}(r, \beta')$ for large N and $P(r, \beta')$ have the same asymptotic behavior for small and large r . This form satisfy the functional equation $\delta P(r) = (1/r^2) \delta P(1/r)$. For large N , the best fit is obtained by tuning only one fitting parameter $C_{\beta', m}$ depending on β' and m (see Table VI for its numerical values. For $m = 7$ case, refer Appendix A). It can be seen from Figs. 1 and 2 that qualitatively these fits are very good.

β'	$c_{\beta'}$	β'	$c_{\beta'}$	β'	$c_{\beta'}$	β'	$c_{\beta'}$
1	2.6597	7	2.2289	14	2.0699	33	2.0300
2	2.4099	8	2.1202	20	2.0493	43	2.0231
3	2.2945	10	2.0970	23	2.0699		
4	2.2289	13	2.0752	26	2.0380		

TABLE II: Values of constants $c_{\beta'}$ used in Eq. (A1).

We also check these best fits with the numerical data quantitatively. Firstly, we calculate the overlap (p) between the probability plots in Figs. 1 and 2 defined as follows:

$$p = 1 - \int |P_{\text{obs}}^k(r, 1, m) - P_{\text{num}}(r, \beta', m)| dr. \quad (11)$$

Secondly, we have studied the cumulative distribution functions corresponding to observed data $P_{\text{obs}}^k(r, 1, m)$

β'	$m = 3$ $C_{\beta', m}$	β'	$m = 4$ $C_{\beta', m}$	β'	$m = 5$ $C_{\beta', m}$	β'	$m = 6$ $C_{\beta', m}$
3	0	1	0	2	-0.8	3	-3
10	-9×10^2	4	-8	7	-60	10	-10^3
20	-2×10^6	8	-300	14	0	20	0
33	-10^{10}	13	-2×10^4	23	10^7	33	-2.5×10^{10}

TABLE III: Values of the parameter $C_{\beta', m}$.

and $P_{\text{num}}(r, \beta')$. We have calculated the maximum absolute difference (d) between these cumulative distributions defined as follows:

$$d = \text{Sup}_{r_i} |F_{\text{obs}}^k(r_i, 1, m) - F_{\text{num}}(r, \beta', m)|, \quad (12)$$

where $F_{\text{obs}}^k(r, 1, m)$ and $F_{\text{num}}(r, \beta', m)$ denotes cumulative distribution functions corresponding respectively to the observed histogram $P_{\text{obs}}^k(r, 1, m)$ and the numerical fit (or postulated function) $P_{\text{num}}(r, \beta', m)$. By definition $0 \leq p, d \leq 1$ and larger (smaller) value of p (d) will indicate that the numerically observed distribution is close to that of the postulated one. The values shown in Tables IV and V gives strong evidences for our claimed conjecture.

k	$m = 3$ p, d	k	$m = 4$ p, d	k	$m = 5$ p, d
3	0.992, 0.00085	2	0.991, 0.00164	3	0.989, 0.00186
6	0.994, 0.00057	4	0.991, 0.00156	6	0.995, 0.00044
9	0.994, 0.00105	6	0.995, 0.00081	9	0.996, 0.00046
12	0.995, 0.00077	8	0.995, 0.00079	12	0.996, 0.00206

TABLE IV: The overlap probability p and the maximum absolute difference d .

k	$m = 6$ p, d	k	$m = 7$ p, d
4	0.991, 0.0009	5	0.991, 0.000112
8	0.996, 0.00046	10	0.995, 0.00096
12	0.996, 0.00054	15	0.997, 0.00094
16	0.996, 0.00138	20	0.996, 0.0013

TABLE V: Same as Table IV.

As a third check for our claim, we have done analysis using only Eq. (3) for $P(r, \beta')$ where no fitting parameter is involved. We numerically find the difference between the cumulative distributions defined as follows:

$$D(\beta') = \sum_i |F_{\text{obs}}^k(r_i, 1, m) - F(r, \beta', m)|, \quad (13)$$

where $F(r, \beta', m)$ denotes the cumulative distribution function corresponding to $P(r, \beta')$. This definition has been used in earlier works [6, 39, 40] in similar kind of analysis. It can be seen that, $D(\beta')$ is minimum for the

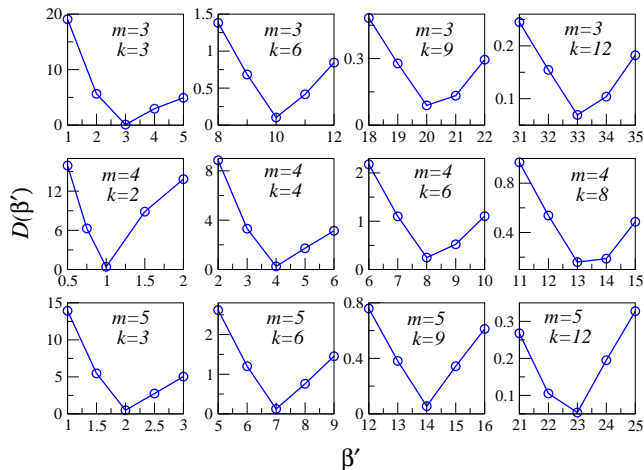


FIG. 3: (Color online) Plot of $D(\beta')$ as a function of β' . The values of m and k in each subfigure are same as that from the corresponding Fig.1.

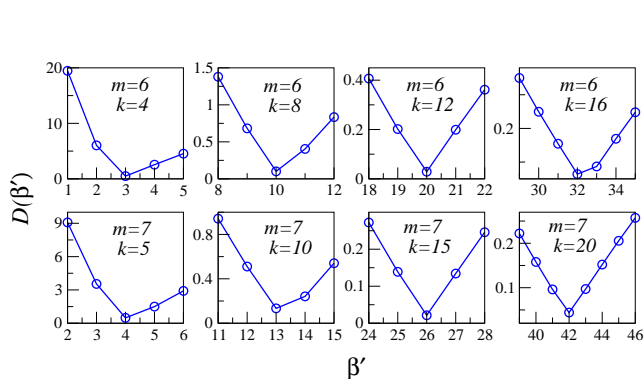


FIG. 4: (Color online) Plot of $D(\beta')$ as a function of β' . The values of m and k in each subfigure are same as that from the corresponding Fig.2.

value of β' for which corresponding $P(r, \beta')$ is the best fit for the observed histogram. The values of k for given m are same as that in Figs. 1 and 2. The results are shown in Figs. 3 and 4 respectively. It can be seen that the minima of $D(\beta')$ in each case coincides remarkably with that of corresponding β' from Figs. 1 and 2.

Now, the numerical simulations supporting the conjectures in Eq. (7) and (8) are presented in Figs. 5 and 6. It can be seen that these figures gives strong numerical evidences for them. We have also tested these conjectures using $D(\beta')$ given in Eq. (13). The results are plotted in the insets of Figs.5 and 6. It can be seen that, the $D(\beta')$ is minimum for the value of β' for which the corresponding $P(r, \beta')$ is the best fit for the observed histograms in Figs.5 and 6, thus supporting the conjectures.

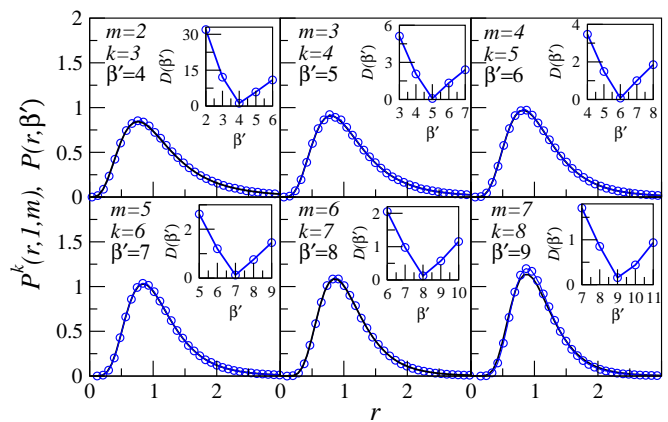


FIG. 5: (Color online) Distribution of the k -th order spacing ratios (circles) for a superposition of m COE spectra. Here, the dimension of the matrices is $N = 8400$. The solid curve corresponds to $P(r, \beta')$ as given in Eq.(7), with $\beta' = k + 1 = m + 2$. Insets: Plot of $D(\beta')$ as a function of β' .

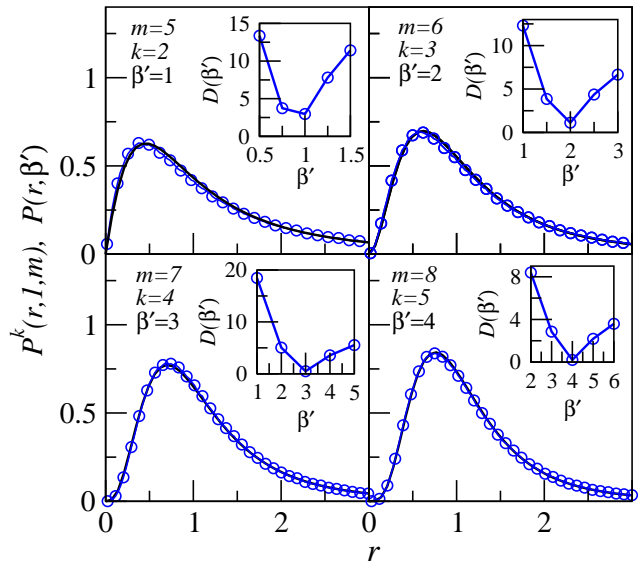


FIG. 6: (Color online) Distribution of the k -th order spacing ratios (circles) for a superposition of m COE spectra. Here, the dimension of the matrices is $N = 8400$. The solid curve corresponds to $P(r, \beta')$ as given in Eq.(8), with $\beta' = k - 1 = m - 4$. Insets: Plot of $D(\beta')$ as a function of β' .

IV. SUMMARY AND CONCLUSIONS

This paper has studied the higher-order spacing ratios of the superposed spectra of COEs. Based on our numerical study, we have conjectured the generalization of the theorem relating COE and CUE ensemble [2, 3]. In the support of this, three different numerical evidences are given. Thus, with our conjecture, one can generate eigenvalues of any circular β -ensemble, where $\beta \geq 3$ and is a positive integer, by superposing $m = \beta + 3$ COEs

and taking every $k = \beta + 1$ -th eigenvalue. The dimension N of the superposing COEs has to be taken such that $N' = mN/(m - 2)$ is an integer, which is also the dimension of the final matrix. Thus, for given β the final matrix can only take dimension in integer multiple of $\beta + 3$. For the special case of $\beta = 3$, one needs to take $m = k = 3$ which implies $N' = N$. Although, matrix model for circular β -ensemble for $\beta \in (0, \infty)$ and for all N' is given in Ref.[5, 18] our result have related all integer-valued β -ensemble to the superposition of COEs in the lines of Refs.[2, 3]. This connection was absent earlier.

Our result also implies that superposing COEs, one again obtains a COE if $m = 4$ and $k = 2$ are taken. It gives one more method of generating a CUE ensemble apart from the earlier one [2, 3] by taking $m = 5$ and $k = 3$. One can also generate CSE using our result if $m = 7$ COEs are superposed and every $k = 5$ -th eigenvalue is chosen. This is yet another method apart of generating CSE from the earlier one [19] where it is shown that set of every second alternate eigenvalue in just a single, even dimensional COE belongs to that of CSE. Thus, one can say that for given positive integer-valued β , the statistical properties of all circular β -ensembles of dimension $i(\beta + 3)$, where i is a positive integer, are reducible to that of COE of dimension $i(\beta + 1)$ alone.

Apart from giving results at the level of jpdf, we have also conjectured two different relations at the level of fluctuations alone. It is conjectured that when the spectra of m number of COEs are superposed then $k = m + 1$ -th ($m \geq 2$) and $k = m - 3$ -th ($m \geq 5$) order spacing ratios distribution converges, in the limit of large matrix dimension, to the corresponding nearest neighbor statis-

tics of $\beta' = m + 2$ and $\beta' = m - 4$ respectively. Similar study was carried recently in Ref.[6] for $k = m$ where $\beta' = m$ was conjectured in the case of GOE. In the same paper this result was used successfully for finding number of symmetries in complex quantum systems. From earlier studies [4, 6, 10] our results can be claimed to be true for GOE in the limit of large matrix dimensions. Our results can provide additional and stringent tests for studying symmetries in these systems [6].

V. ACKNOWLEDGMENTS

Author is grateful to M. S. Santhanam and Harshini Tekur for discussions at various stages of this paper. The results presented in the paper are based on the computations using *Mathematica 9* in Vikram-100, the 100TFLOP HPC Cluster at Physical Research Laboratory, Ahmedabad, India.

Appendix A: Values of constants $c_{\beta'}$ and the parameter $C_{\beta', m}$.

Exact values of constants $c_{\beta'}$ is calculated using the normalization condition $\int_0^\infty \delta P_{\text{fit}}(r, \beta') dr = 0$ where

$$\delta P_{\text{fit}}(r, \beta', m) = \frac{C_{\beta', m}}{(1+r)^2} \left[\left(r + \frac{1}{r} \right)^{-\beta'} - c_{\beta'} \left(r + \frac{1}{r} \right)^{-(\beta'+1)} \right]. \quad (\text{A1})$$

The values are given as follows:

$$c_1 = \frac{2(\pi - 2)}{4 - \pi}, \quad c_2 = \frac{4(4 - \pi)}{3\pi - 8}, \quad c_3 = \frac{6(8 - 3\pi)}{(9\pi - 32)}, \quad c_4 = \frac{8(9\pi - 32)}{45\pi - 128}, \quad c_7 = \frac{35\pi/4096 - 1/40}{1/70 - 35\pi/8192}, \quad (\text{A2})$$

$$c_8 = \frac{65536 - 19600\pi}{11025\pi - 32768}, \quad c_{10} = \frac{262144 - 79380\pi}{43659\pi - 131072}, \quad c_{13} = \frac{54525952 - 18036018\pi}{9018009\pi - 29360128}, \quad (\text{A3})$$

$$c_{14} = \frac{16777216 - 5153148\pi}{2760615\pi - 8388608}, \quad c_{20} = \frac{274877906944 - 85336948840\pi}{44801898141\pi - 137438953472}, \quad (\text{A4})$$

$$c_{23} = \frac{25288767438848 - 8226517131378\pi}{-13194139533312 + 4113258565689\pi}, \quad c_{26} = \frac{281474976710656 - 87890140292500\pi}{45635265151875\pi - 140737488355328}, \quad (\text{A5})$$

$$c_{33} = \frac{66(2980705490751054825\pi - 9223372036854775808)}{313594649253062377472 - 98363281194784809225\pi} \quad \text{and} \quad (\text{A6})$$

$$c_{43} = \frac{86(-604462909807314587353088 + 194656659282135509820075\pi)}{26596368031521841843535872 - 8370236349131826922263225\pi}. \quad (\text{A7})$$

[1] M. A. Nielsen and I. L. Chuang, *Quantum computation and quantum information* (Cambridge University Press,

Cambridge, 2000).

[2] F. J. Dyson, *J. Math. Phys.* **3**, 166 (1962).

β'	$m = 7$ $C_{\beta',m}$
4	-11
13	-1.8×10^4
26	-10^8
43	8×10^{13}

TABLE VI: Values of the parameter $C_{\beta',m}$ for $m = 7$.

- [3] J. Gunson, *Journal of Mathematical Physics* **3**, 752 (1962).
- [4] M. L. Mehta, *Random Matrices* (Elsevier Academic Press, 3rd Edition, London, 2004).
- [5] G. W. Anderson, A. Guionnet, and O. Zeitouni, *An introduction to random matrices*, vol. 118 (Cambridge university press, 2010).
- [6] S. H. Tekur and M. Santhanam, arXiv preprint arXiv:1808.08541 (2018).
- [7] K. Brading and E. Castellani, *Symmetries in physics: philosophical reflections* (Cambridge University Press, 2003).
- [8] S. Corry, *Symmetry and Quantum Mechanics* (Chapman and Hall/CRC, 2016).
- [9] D. J. Gross, *Proceedings of the National Academy of Sciences* **93**, 14256 (1996).
- [10] P. J. Forrester, *Log-Gases and Random Matrices* (Princeton University Press, Princeton and Oxford, 2010).
- [11] I. Dumitriu and A. Edelman, *Journal of Mathematical Physics* **43**, 5830 (2002).
- [12] W. Buijsman, V. Cheianov, and V. Gritsev, arXiv preprint arXiv:1807.05075 (2018).
- [13] O. Bohigas, M. J. Giannoni, and C. Schmit, *Phys. Rev. Lett.* **52**, 1 (1984).
- [14] M. V. Berry and M. Tabor, *Proc. R. Soc. Lond. A* **356**, 375 (1977).
- [15] F. J. Dyson, *J. Math. Phys.* **3**, 140 (1962).
- [16] G. Akemann, J. Baik, and P. Di Francesco, *The Oxford handbook of random matrix theory* (Oxford University Press, 2011).
- [17] F. Mezzadri, *Notices of the AMS* **54**, 592 (2007).
- [18] R. Killip and I. Nenciu, *International Mathematics Research Notices* **2004**, 2665 (2004).
- [19] M. L. Mehta and F. J. Dyson, *J. Math. Phys.* **4**, 713 (1963).
- [20] C. E. Porter, *Statistical Theories of Spectra: Fluctuations* (Academic Press, New York, 1965).
- [21] V. Oganessian and D. A. Huse, *Phys. Rev. B* **75**, 155111 (2007).
- [22] Y. Y. Atas, E. Bogomolny, O. Giraud, and G. Roux, *Phys. Rev. Lett.* **110**, 084101 (2013).
- [23] Y. Atas, E. Bogomolny, O. Giraud, P. Vivo, and E. Vivo, *Journal of Physics A: Mathematical and Theoretical* **46**, 355204 (2013).
- [24] V. Oganessian, A. Pal, and D. A. Huse, *Phys. Rev. B* **80**, 115104 (2009).
- [25] A. Pal and D. A. Huse, *Phys. Rev. B* **82**, 174411 (2010).
- [26] S. Iyer, V. Oganessian, G. Refael, and D. A. Huse, *Phys. Rev. B* **87**, 134202 (2013).
- [27] E. Cuevas, M. Feigel'Man, L. Ioffe, and M. Mezard, *Nature communications* **3**, 1128 (2012).
- [28] G. Biroli, A. Ribeiro-Teixeira, and M. Tarzia, arXiv preprint arXiv:1211.7334 (2012).
- [29] C. Chen, F. Burnell, and A. Chandran, *Phys. Rev. Lett.* **121**, 085701 (2018).
- [30] L. F. Santos and M. Rigol, *Phys. Rev. E* **81**, 036206 (2010).
- [31] C. Kollath, G. Roux, G. Biroli, and A. M. Läuchli, *Journal of Statistical Mechanics: Theory and Experiment* **2010**, P08011 (2010).
- [32] M. Rigol and L. F. Santos, *Phys. Rev. A* **82**, 011604 (2010).
- [33] L. F. Santos and M. Rigol, *Phys. Rev. E* **82**, 031130 (2010).
- [34] M. Collura, H. Aufderheide, G. Roux, and D. Karevski, *Phys. Rev. A* **86**, 013615 (2012).
- [35] E. Tarquini, G. Biroli, and M. Tarzia, *Phys. Rev. Lett.* **116**, 010601 (2016).
- [36] N. Chavda, H. Deota, and V. Kota, *Physics Letters A* **378**, 3012 (2014).
- [37] V. Kota and N. Chavda, *International Journal of Modern Physics E* **27**, 1830001 (2018).
- [38] S. H. Tekur, S. Kumar, and M. S. Santhanam, *Phys. Rev. E* **97**, 062212 (2018).
- [39] S. H. Tekur, U. T. Bhosale, and M. S. Santhanam, *Phys. Rev. B* **98**, 104305 (2018).
- [40] U. T. Bhosale, S. H. Tekur, and M. S. Santhanam, *Phys. Rev. E* **98**, 052133 (2018).
- [41] P. J. Forrester and E. M. Rains, *Probability theory and related fields* **130**, 518 (2004).
- [42] P. J. Forrester, *Communications in mathematical physics* **285**, 653 (2009).
- [43] F. J. Dyson, *J. Math. Phys.* **3**, 140 (1962).